

---

---

NANOTECHNOLOGIES  
IN OPTICS AND ELECTRONICS

---

---

## Analysis of the Contact Probe Mechanism for Micro-Coordinate Measuring Machines

K.-Ch. Fan<sup>a,b</sup>, F. Cheng<sup>b</sup>, W.-T. Pan<sup>b</sup>, and R. Li<sup>b</sup>

<sup>a</sup>*School of Instrument Science and Optoelectronic Engineering, Hefei University of Technology,  
Tunxi Rd. 193, Hefei, Anhui, China 230009*

<sup>b</sup>*Department of Mechanical Engineering, National Taipei University of Technology, 1, Sec. 3,  
Chung-Hsiao E. Rd., Taipei, Taiwan 106*  
*E-mail: fan@ntu.edu.tw*

Received February 18, 2020

**Abstract**—High precision contact scanning probes for measuring miniature components on micro- and nano-coordinate measuring machines requires sensitive mechanisms. This paper analyzes the mechanism of a developed contact probe in order to find its optimal dimensions. The contact probe is composed of a fiber stylus with a ball tip, a mechanism with a wire-suspended floating plate, and focus sensors. The wires experience elastic deformation when a contact force is applied. The probe mechanism with a four-wire floating plate is studied. Stiffness analysis is carried out using the theory of elasticity. It is found that, with a proper stylus length, a contact probe with uniform stiffness can be designed.

**DOI:** 10.3103/S8756699010040060

*Key words:* contact probe, floating plate, stiffness, coordinate measuring machines.

### INTRODUCTION

The increasing demands of industry for higher accuracy measurements of micro systems has led to the development of the field of micro- and nanodimensional metrology [1]. During the past decade, several micro- or nano-coordinate measuring machines (CMM) that can measure meso- to micro-scaled parts with nanometer resolution have been developed. They are equipped with noncontact probes [2, 3] or contact probes [4–6]. Although noncontact probes feature fast surface scanning, for any CMM, however, the need for 3D contact probes is indispensable due to their capability to measure most fundamental geometries, such as line, plane, circle, sphere, cone, etc. A variety of contact probe systems have been designed for micro- and nano-CMM, such as silicon-based [7], flexure structure-based [5, 6], fiber Bragg grating type [8], boss membrane structures [9], suspension plate [10, 11] and others [12].

A scanning contact probe normally consists of an elastic mechanism and several sensors in order to detect the movement of the probe tip in all directions. The contact force should be small, normally less than 1 mN, and the tip ball radius should be small, normally less than 300  $\mu\text{m}$ , and the stiffness should be low, normally less than 1 mN, and equal in all directions [6, 10].

A new analog tactile probe was developed in [11]. It is composed of a monolithic fiber stylus with a ball tip, a wire-suspended floating plate as the main mechanism, and some focus sensors [11]. Although this probe meets most of the requirement, its stiffness is not uniform in different directions. This paper deals with a detailed investigation of the design of the probe mechanism. Stiffness analysis is carried out using the theory of elasticity and finite element analysis. It is found that with a proper stylus length, a contact probe with uniform stiffness can be designed.

In Section 1, the design principle and structure of the scanning contact probe for two types of mechanism will be explained. Stiffness analysis using the theory of elasticity is described in Section 2.

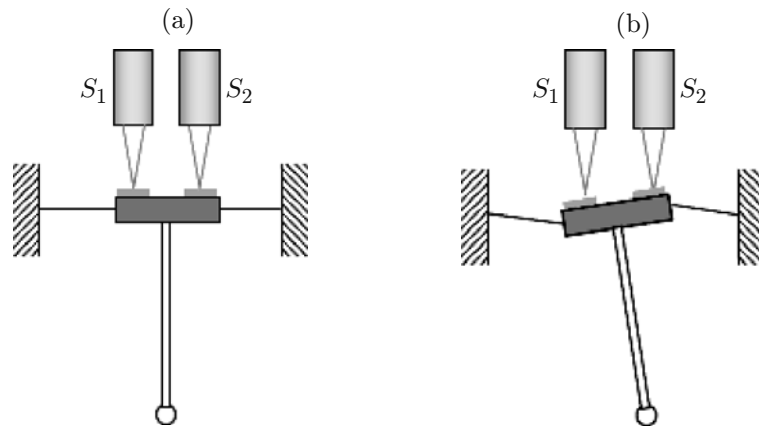


**Fig. 1.** Principle of the contact probe: (a) in the rest mode; (b) in the contact mode.

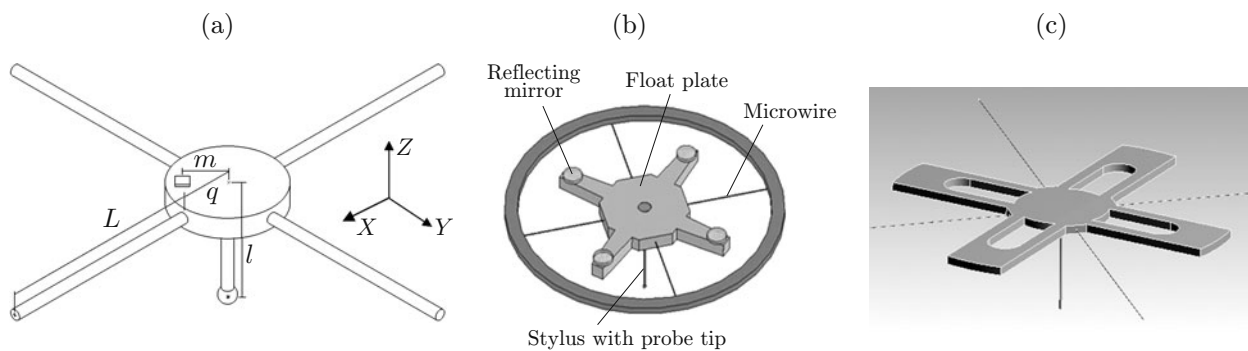


**Fig. 2.** Four-wire floating plate: (a) circular plate; (b) plate with extended arms; (c) plate with light weight design.

## PROBE DESIGN

### 1.1. Design Principle

A complete contact probe normally consists of three modules, namely: a stylus with a ball tip, a mechanical mechanism with a low moment of inertia which is sensitive to the movement of the ball tip, and sensitive sensors to detect the movement of the mechanism. Figure 1 shows the design principle of the proposed contact probe. The probe stylus is fabricated from an optical fiber by melting and solidification process [13]. With proper selection of process parameters using the Taguchi method, this monolithic ball tip stylus can have very good sphericity [14]. The stylus is fixed to a floating plate, which is suspended by evenly distributed wires connected to the probe housing. The contact force causes the floating plate to tilt and move vertically as a rigid body motion while the wires experience elastic deformations. Plate motion is detected by focus sensors on the top of mirrors mounted at proper positions of the floating plate. In planar motion, signals of two sensors  $S_1$  and  $S_2$  are converted to displacements of the ball in the  $X$  and  $Y$  directions. In spatial motion, at least three sensors are needed to calculate ball displacements in three directions. The shift of the ball can be obtained within the sensor's measuring range. This is a kind of scanning contact probe.

### 1.2. Probe Mechanism Design

In this paper, we analyze a four-wire type probe mechanism. There are a variety of design configurations, three of which are shown in Fig. 2. The first type is a circular floating plate suspended evenly by four wires (or thin rods) (Fig. 2a). The second type has extended arms for mirror mounting so as to be more sensitive to shifts of the tip ball (Fig. 2b). The third type has a reduced moving weight to provide a lower moment of inertia (Fig. 2c). Mirrors should be placed at the arm end for displacement magnification. It is noted that the floating plate is considered only as a moving rigid body whereas the wires are elastically deformed.

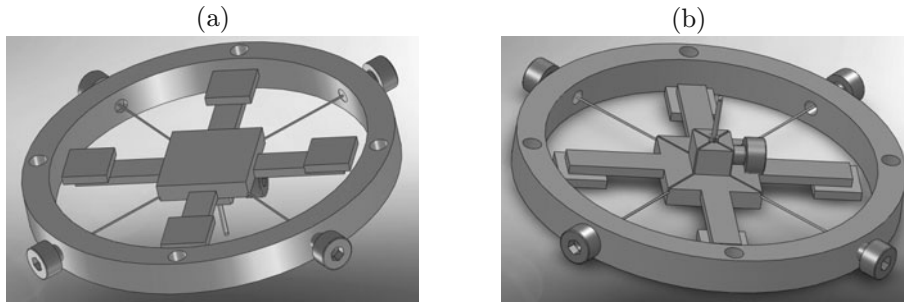


**Fig. 3.** Physical probe mechanism: (a) top view; (b) bottom view.

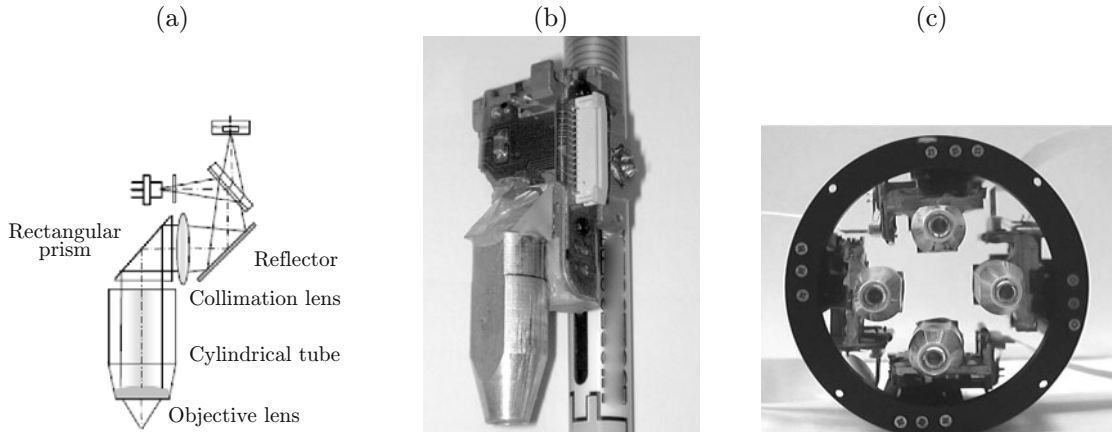


**Fig. 4.** Focus sensors in the probe: (a) optical system; (b) photograph of one sensor; (c) a photograph of four assembled sensors.

Features of the four-wire design are its symmetry and balance in the  $X$  and  $Y$  directions. Although three sensors are sufficient to calculate the spatial motion of the tip ball, the fourth sensor can help verify the accuracy. An example of the physical four-wire mechanism design is presented in Fig. 3. It is seen that each wire is embedded in a groove in the plate, which creates a built-in boundary condition, and its initial tension can be adjusted by a screw. The stylus length can also be changed by a setting screw. Four reflecting mirrors are mounted on the corresponding arm ends and should be adjusted to a common plane during assembly.

### 1.3. Probe Assembly

In practice, all components must be made as small as possible to fit the dimension of micro-CMM. The floating plate is thin. The major part affecting the probe size is the focus sensor. In the present study, we used a focus sensor with a DVD pickup head. Being a mass production device, the pickup head is inexpensive but very accurate. The laser focus probe uses the astigmatism principle [15]. Displacement of the reflecting mirror causes a focus error signal (FES) of the embedded quadrant photodetector. This FES performs an extremely linear curve within the focus range with a resolution of 1 nm [16]. The pickup head is reconfigured by a special design. As shown in Fig. 4a, the upper right part is the pickup head, where its objective lens is detached and moved to the end of the cylindrical tube. A prism is used to deflect the laser beam downward. Figure 4b shows a photograph of one sensor and its size relative to a ball pen. Figure 4c shows a photograph of four assembled sensors. A photograph of the assembled probe head without the mounting of the probe mechanism is given in Fig. 5a, and a CAD drawing of the complete probe of the four-wire type in Fig. 5b.

## 2. DESIGN ANALYSIS OF THE PROBE MECHANISM

The main task of the floating plate is to provide a stable rest position and a tilt angle of the probe relative to the contact force in three orthogonal directions. The shape and dimension of the floating plate, as well as the length and diameter of the micro wire, are determined according to the required tip ball movement

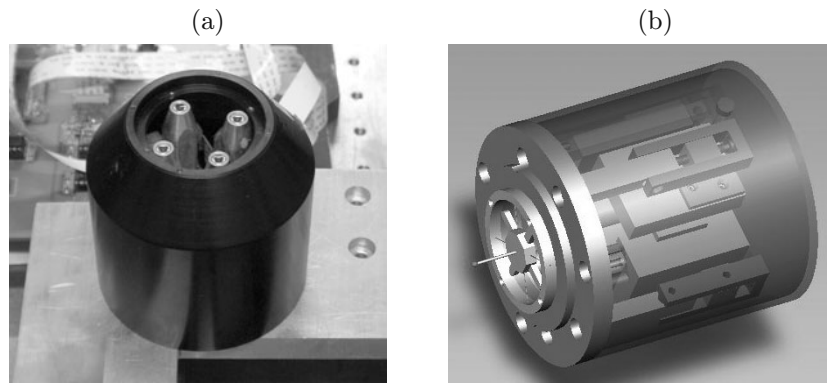


**Fig. 5.** Assembled probe head: (a) without probe mechanism; (b) complete probe.

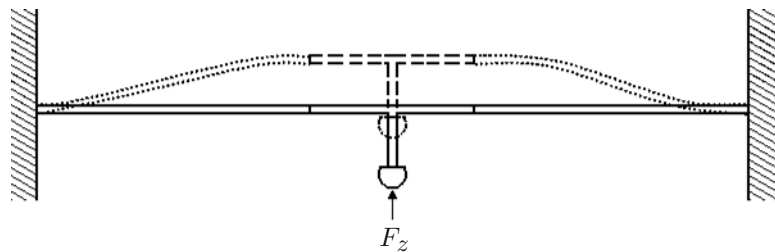


**Fig. 6.** Mechanism deflection under a contact force in the  $Z$  direction.

and contact forces. The probing force is normally required to be less than 1 mN. The dimension of the mechanism can be calculated by the finite element method, in order to obtain an optimum geometry. Due to its symmetrical geometry, the force-motion characteristics will be symmetric in the  $X$ - $Y$  plane. In order to analyze the response of the displacement to the contact force, the structure of a simplified circular plate (Fig. 2a) needs to be taken into account. Mechanical behavior under a contact force can be analyzed using the theory of elasticity.

### 2.1. Deformation under Vertical Contact Force

The deflection behavior under an applied force can be modeled by a cross-sectional view of the wire-plate-stylus structure. When a vertical force  $F_Z$  is applied to the ball tip, all wires are deflected symmetrically in the  $Z$  direction, as shown in Fig. 6. Since the wires are imbedded in the floating plate (each wire is treated as a slender thin beam), the slope at the free end of the beam should be zero. Free body diagrams of the floating plate and the right wire are shown in Fig. 7. Taking the free body diagram of the right wire into account, the shear force  $P$  and the bending moment  $M$  are reactions of the plate to the load. Due to the geometrical symmetry of four wires,  $P = F_Z/4$ . At this moment,  $M$  is unknown and has to be found.

From the theory of elasticity, the vertical displacement and the slope at the free end under each load can be summarized (see table, where  $L$  is the wire length,  $I$  is the moment of inertia of the wire, and  $E$  is Young's modulus of the wire material).

At the boundary of the wire end, the slope must be zero, so that  $\theta_1 = \theta_2$ . Therefore,  $M$  can be found as

$$M = (PL)/2. \quad (1)$$

Because the floating plate is treated as a moving rigid body, the total displacement at the wire end  $\delta_Z$  is the same as the tip ball displacement:

$$\delta_{b,Z} = \delta_1 - \delta_2. \quad (2)$$

Substituting  $\delta_1$  and  $\delta_2$  and  $M$  into Eq. (2), we can find the displacement of the tip ball under a contact force  $F_Z$ . For the case of four-wire suspension ( $P = F_Z/4$ ), we obtain

$$\delta_{b,Z} = (F_Z L^3)/(48EI). \quad (3)$$

We note that this derivation is also applicable to any  $N$ -wire suspension. Thus, the more the suspension wires, the larger the probe stiffness in the  $Z$  direction.

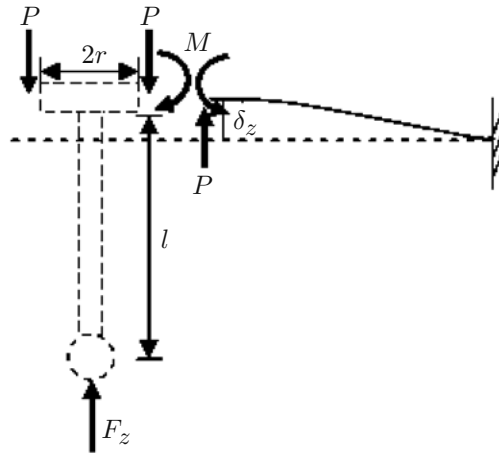


**Fig. 7.** Free body diagrams for the floating plate and the right wire under a vertical force  $F_z$  applied to the tip ball.

Elastic behavior at the wire end under various loads		
Load	Deflection	Slope
$P$	$\delta_1 = (PL^3)/(3EI)$	$\theta_1 = (PL^2)/(2EI)$
$M$	$\delta_2 = (ML^2)/(2EI)$	$\theta_2 = (ML)/(EI)$

2.2. Deformation under a Horizontal Contact Force

When a horizontal force is applied to the ball tip, the two wires located in the same direction are deflected in the  $Z$  direction in an symmetric manner, while the other two wires are twisted. The same is true for a contact force in the  $X$  direction. If a contact force is applied to any direction in the horizontal plane, it can be considered as two partial orthogonal forces acting on the tip ball in the  $X$  and  $Y$  directions simultaneously. For simplicity, the case of  $F_Y$  force is analyzed. Figure 8a shows the structure before motion, and Fig. 8b shows the shape of elastic deformation, where the moment  $M$  is the multiplication of the force  $F$  and the stylus length  $l$ . A free body diagram for the floating plate is given in Fig. 9a, and a free body diagram for the right wire in Fig. 9b.

Let the deflection of the wire be  $y$ . From the basic beam deflection equations we have

$$EIy'''' = 0. \tag{4}$$

Integrating this equation four times, we obtain

$$EIy = \frac{1}{6} C_1 x^3 + \frac{1}{2} C_2 x^2 + C_3 x + C_4, \tag{5}$$

where  $C_1, C_2, C_3,$  and  $C_4$  are constants.

The boundary conditions are  $EIy''' = P, EIy'' = -M, y'(0) = \theta, y(0) = \delta, y'(L) = 0,$  and  $y(L) = 0;$  therefore,  $C_1 = P, C_2 = -M, C_3 = EI\theta,$  and  $C_4 = EI\delta.$  As a result, we have

$$P = \frac{12EI\delta + 6EI\theta L}{L^3}, \tag{6}$$

$$M = \frac{6EI\delta + 4EI\theta L}{L^2}. \tag{7}$$

As follows from Fig. 9a, the tip ball movement can be approximated by relations

$$\delta_{b,Y} = l\theta, \quad \delta = (r/l)\delta_{b,Y}, \tag{8}$$

$$F_Y l = 2M + 2rP. \tag{9}$$

Therefore, substitution of Eqs. (6)–(8) into Eq. (9) yields

$$F_Y = \frac{8EI}{l^2 L^3} (3rL + L^2 + 3r^2)\delta_{b,Y}, \tag{10}$$

where  $r$  is the plate radius.

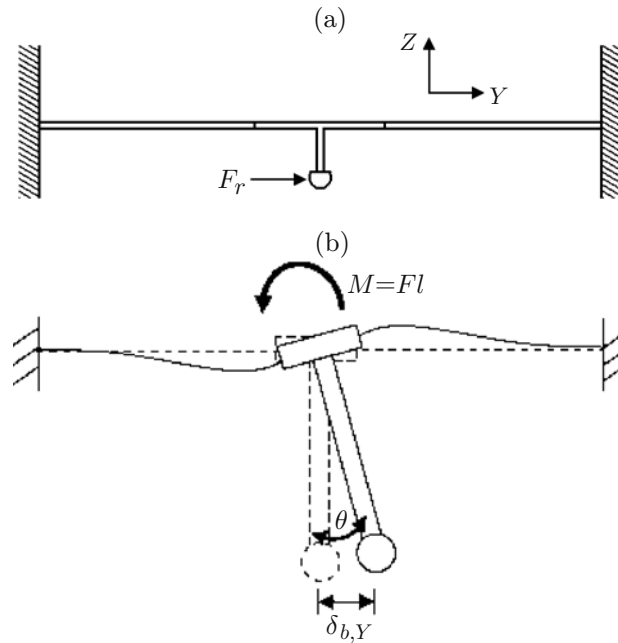


Fig. 8. Mechanism under a contact force in the Y direction: (a) before motion; (b) after motion.

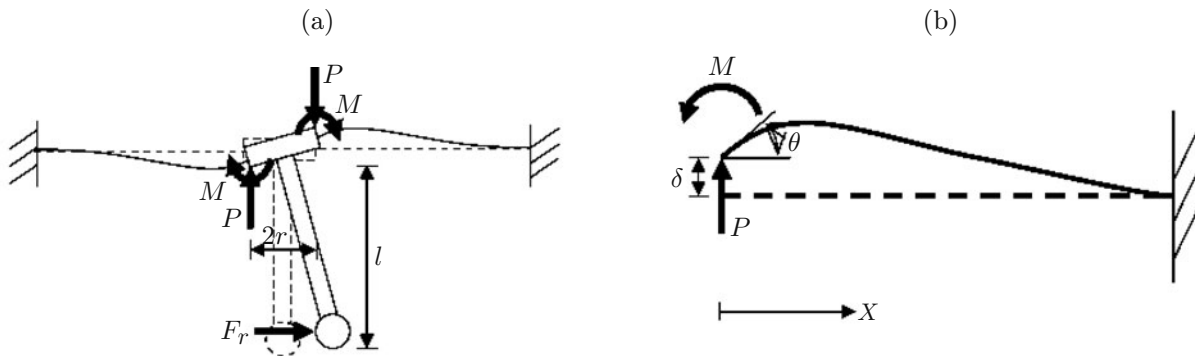


Fig. 9. Free body diagrams under of a horizontal force  $F_Y$  for the floating plate (a) and the right wire (b).

Since the probe mechanism is symmetrical in the horizontal plane, the same result can be obtained for the contact force in the X direction. The displacement-to-force relationship can be derived from Eqs. (3) and (10):

$$\begin{bmatrix} \delta_{b, X} \\ \delta_{b, Y} \\ \delta_{b, Z} \end{bmatrix} = \begin{bmatrix} C_1 & 0 & 0 \\ 0 & C_1 & 0 \\ 0 & 0 & C_2 \end{bmatrix} \begin{bmatrix} F_{b, X} \\ F_{b, Y} \\ F_{b, Z} \end{bmatrix}, \tag{11}$$

where

$$C_1 = \frac{l^2 L^3}{8EI(3r^2 + 3rL + L^2)}; \quad C_2 = \frac{L^3}{48EI}.$$

We note that  $r$  here is the same as  $q$  in Fig. 2a. The stiffness of the probe mechanism is the inverse of  $C$  in the corresponding direction. The parameters affecting the stiffness are the wire length  $L$ , the stylus length  $l$ , the plate radius  $r$ , the moment of inertia of the wire  $I$ , and Young's modulus of the wire material  $E$ . It is seen that, with proper selection of the dimension of floating mechanism, it is possible to design a probe mechanism of this four-wire suspended floating plate type with constant stiffness in all directions, i.e.,  $C_1 = C_2$ .

## CONCLUSIONS

This paper describes the design of a contact scanning probe for a micro-CMM. This innovative probe combines a probe stylus, a mechanical floating mechanism with four-wire suspension and four focus sensors made from DVD pickup heads, resulting in a high resolution with low cost. A novel suspension mechanism is proposed to increase the sensitivity, and the stiffness of the structure was calculated using the elasticity theory. From the deformation analysis, it is possible to design a probe mechanism of this four-wire floating plate type with constant stiffness in all directions.

The work reported is part of a research program funded by the Natural Science Foundation of China (Grant Nos. 50875073 and 50420120134) and the National Science Council of Taiwan (Grant No. NSC97-2221-E-002-092).

## REFERENCES

1. P. McKeown, "Nanotechnology—Special Article," in *Proc. of the Nano-Metrology in Precision Engineering, Hong Kong* (1998), pp. 5–55.
2. K. C. Fan, Y. T. Fei, X. F. Yu, et al., "Development of a Low-Cost Micro-CMM for 3D Micro- and Nanomeasurements," *Meas. Sci. Technol.* **17** (3), 524–532 (2006).
3. G. Jäger, E. Manske, and T. Hausotte, "Nanopositioning and Measuring Machine," in *Proc. of the 2nd EUSPEN Int. Conf.*, (Turin, 2001), Vol. 1, pp. 290–293.
4. K. Takamasu, K. R. Furutani, and S. Ozono, "Development of Nano-CMM (Coordinate Measuring Machine with Nanometer Resolution)," in *Proc. of the XIV IMEKO World Congress* (Finland, 1997), Vol. 8, pp. 34–39.
5. G. N. Peggs, A. J. Lewis, and S. Oldfield, "Design for a Compact High-Accuracy CMM," *Ann. CIRP.* **48** (1), 417–420 (1999).
6. A. Küng, F. Meli, and R. Thalmann, "Ultraprecision Micro-CMM Using a Low Force 3D Touch Probe," *Meas. Sci. Technol.* **18** (2), 319–327 (2007).
7. H. Haitjema, W. O. Pril, and P. Schellekens, "Development of a Silicon-Based Nanoprobe System for 3-D Measurements," *Ann. CIRP* **50** (1), 365–368 (2001).
8. H. Ji, H. Y. Hsu, L. X. Kong, and A. B. Wedding, "Development of a Contact Probe Incorporating a Bragg Grating Strain Sensor for Nano Coordinate Measuring Machines," *Meas. Sci. Technol.* **20** (9), 095304 (2009).
9. A. Tibrewala, A. Phataralaoha, and S. Buttgenbach, "Development, Fabrication and Characterization of a 3D Tactile Sensor," *J. Micromech. Microeng.* **19** (12), 125005 (2009).
10. C. L. Chu and C. Y. Chiu, "Development of a Low Cost Nanoscale Touch Trigger Probe Based on Two Commercial DVD Pick-up Heads," *Meas. Sci. Technol.* **18** (7), 1831–1842 (2007).
11. K. C. Fan, F. Cheng, W. L. Wang, et al., "A Scanning Contact Probe for a Micro Coordinate Measuring Machines (CMM)," *Meas. Sci. Technol.* **21** (5), 054002 (2010).
12. A. Weckenmann, G. Peggs, and J. Hoffmann, "Probing Systems for Dimensional Micro- and Nano-Metrology," *Meas. Sci. Technol.* **17** (3), 504–509 (2006).
13. K. C. Fan, H. Y. Hsu, P. Y. Hung, et al., "Experimental Study of Fabricating a Micro Ball Tip on the Optical Fiber," *J. Opt. A: Pure Appl. Opt.* **8** (9), 782–787 (2006).
14. K. C. Fan, W. L. Wang, and H. S. Chiou "Fabrication Optimization of a Micro-Spherical Fiber Probe with the Taguchi Method," *J. Micromech. Microeng.* **18** (1), 0150111 (2008).
15. K. C. Fan, C. Y. Lin, and L. H. Shyu, "Development of a Low Cost Focusing Probe for Profile Measurement," *Meas. Sci. Technol.* **11** (1), 1–7 (2000).
16. K. C. Fan, G. Jäger, Y. J. Chen, and R. Mastyllo, "Development of a Non-Contact Optical Focus Probe with Nanometer Accuracy," in *Proc. of the 7th EUSPEN Int. Conf., Bremen, Germany, 2007*, pp. 278–281.